Contents lists available at SciOpen

Food Science and Human Wellness

journal homepage: https://www.sciopen.com/journal/2097-0765

China Food Publishing Co.

L-Theanine/*α*-ketoglutarate/Nrf2 axis promotes exercise-mediated amelioration of nonalcoholic steatohepatitis in mice

Wangjing Mu[a,b,c], Min Chen[a,b,c], Jieying Zhu[a,b,c], Hongyang Luo[a,b,c], Yang Li[a,b,c], Shan Li[a,b,c], Linjing Yan[a,b,c], Ruoying Li[a,b,c], Liang Guo[a,b,c,*]

[a] *School of Exercise and Health, Collaborative Innovation Center for Sports and Public Health, Shanghai University of Sport, Shanghai 200438, China*
[b] *Shanghai Frontiers Science Research Base of Exercise and Metabolic Health, Shanghai University of Sport, Shanghai 200438, China*
[c] *Key Laboratory of Exercise and Health Sciences of the Ministry of Education, Shanghai University of Sport, Shanghai 200438, China*

ARTICLE INFO

Article history:
Received 3 January 2024
Received in revised form 19 February 2024
Accepted 26 March 2024

Keywords:
DNA demethylation
Exercise
L-Theanine
Nonalcoholic steatohepatitis
Nrf2

ABSTRACT

L-Theanine (LTA) is a non-protein amino acid mainly found in tea plants with many beneficial effects. Exercise exerts a wide range of benefits in metabolic health. Here, we show that exercise or gastric lavage intervention on mice with LTA improves diet-induced nonalcoholic steatohepatitis (NASH) in mice. Meanwhile, combinatory therapy shows that exercise and LTA synergistically improve obesity-related metabolic disorders and NASH phenotypes, including hepatic steatosis, inflammation, cell death and oxidative stress. *In vivo* studies indicate that LTA inhibits free fatty acid (FFA)-induced hepatocyte injury, including steatosis, oxidative stress and apoptosis. Knockdown of *Nrf2* blunts the role of LTA in inhibiting FFA-induced hepatocyte oxidative stress and dysfunction. Mechanistically, LTA increases the *α*-ketoglutarate (*α*-KG) level in hepatocytes, which increases the transcription of *Nrf2* by inducing active DNA demethylation on its promoter. Moreover, LTA promote the above *α*-KG/Nrf2 axis in synergy with exercise, thereby more efficiently inhibiting hepatic oxidative stress and ameliorating diet-induced NASH in mice. Our results suggest that, through promoting the *α*-KG/Nrf2 axis-mediated anti-oxidative pathway, the combination of LTA and exercise may provide an effective measure for the prevention and control of NASH.

1. Introduction

Nonalcoholic fatty liver disease (NAFLD) comprises a spectrum of hepatic disorders arising from the disproportionate buildup of triglycerides (TG) within the liver, occurring without substantial alcohol consumption[1]. The buildup of lipids in the liver can lead to the progression of hepatic steatosis into chronic liver damage, accompanied by inflammation and fibrosis. Nonalcoholic steatohepatitis (NASH) represents a phase in the progression of NAFLD, characterized by hepatocyte steatosis exceeding 5%, accompanied by intralobular inflammation and hepatocyte ballooning, with or without fibrosis[2-3]. Metabolic syndrome is significantly associated with the development of NASH[4-8].

Surveys indicate that approximately 25% of individuals worldwide are affected by NAFLD, with 20% of these individuals progressing to NASH. Over time, 5% of those with NASH experience spontaneous reversal, while 4% of NAFLD patients and 20% of NASH patients advance to cirrhosis[9]. NASH is also linked to an elevated risk of cardiovascular disease[10], leading to increased

* Corresponding author at: School of Exercise and Health, Shanghai University of Sport, Shanghai 200438, China.
E-mail address: guoliang@sus.edu.cn (L. Guo)
Peer review under responsibility of Beijing Academy of Food Sciences.

SciOpen Publishing services by Tsinghua University Press

http://doi.org/10.26599/FSHW.2024.9250242

cardiovascular and liver-related mortality[11-13]. Consequently, NASH has become the fastest-growing indication for liver transplantation[14]. Projections suggest a significant rise in the number of people with NASH, including in countries like China, the United States, and Germany, by the year 2030[15]. Currently, no therapeutics for NASH have received approval for marketing through randomized controlled trials to confirm their efficacy and safety. The escalating incidence and mortality rates associated with NASH present a substantial burden on both families and society. In summary, NASH has surfaced as a notable public health concern.

Exercise plays a pivotal role in improving metabolism and combating diseases, exerting significant impacts on physiological well-being[16-17]. In the absence of approved drug therapies, exercise emerges as a viable and currently effective approach for NASH treatment. A notable link exists between the manifestation of metabolic syndrome and the onset of NASH. Exercise-induced enhancement of peripheral insulin resistance plays a crucial role in reducing the excessive delivery of free fatty acids and glucose to the liver, thereby mitigating free fatty acid synthesis. Exercise exerts a multifaceted impact on the liver metabolism, promoting increased fatty acid oxidation, curbing fat synthesis, and preventing excessive fatty acid accumulation[18-19]. Moreover, individuals engaging in physical activity for at least 60 min per week experienced notable improvement in fasting blood glucose, fasting insulin, homeostasis model assessment (HOMA), and various metabolic risk factors[20]. Notably, improvement in serum levels of liver enzymes was more pronounced across all physical activity categories compared to the sedentary group. Exercise has also demonstrated efficacy in reducing pre-existing NASH and fibrosis[21]. In a study involving mice subjected to a high-fat diet (HFD) to induce severe NASH or fibrosis, exercise demonstrated significant reversal of hepatic steatosis and inflammation, with a tendency to improve hepatic fibrosis. The hepatic fibrosis induced by HFD, characterized by collagen deposition in distinctive patch-like structures, was mitigated by exercise, as reflected in reduced histological collagen content in the liver. In a study involving mice, the exercise group demonstrated a significant decrease in plasma alanine aminotransferase (ALT), which is a marker of liver damage. Similar positive effects of exercise on decreasing serum levels of liver enzymes have been observed in humans, with serum ALT levels decreasing during 12 months of regular exercise in NAFLD patients[22]. Compelling evidence supports the positive impact of moderate-intensity aerobic exercise on normalizing serum ALT levels in patients with NASH, as demonstrated in a randomized controlled trial, where 98.3% of NASH patients exhibited central obesity, and 20.3% had metabolic syndrome[23]. Among the 44 patients consistently adhering to the exercise program, a notable reduction in mean serum aspartate aminotransferase (AST) and ALT values was observed. Yet, the detailed mechanisms responsible for the beneficial effects of exercise on alleviating NASH have not been fully elucidated.

L-Theanine (LTA) is predominantly biosynthesized in the roots of tea plants[24]. Subsequently, it is transported to shoots for hydrolysis. The absorption of LTA occurs in small intestinal villi epithelial cells *via* sodium-coupled transporter proteins[25-26]. Furthermore, the benefits extend beyond the liver, as LTA-induced improvement in insulin sensitivity and metabolic parameters are distributed across various tissues, including the liver, brain, and kidneys[27]. In recent years, there has been a growing focus on the health benefits attributed to LTA. Reports indicated that LTA consumption yields numerous therapeutic effects, such as enhancement in brain and gastrointestinal function, increasing efficacy of anti-cancer drugs, antihypertensive effects, and improved immune function[28]. Moreover, LTA has demonstrated positive effects on various liver disorders, encompassing simple fatty liver[29], alcoholic fatty liver disease[30], and doxorubicin-induced acute liver damage[31]. However, its protective role against NASH remains poorly understood.

In the present study, the possible protective effects of LTA, exercise and the combination of both on diet-induced NASH in mice were analyzed. Exercise or gastric gavage of LTA was found to improve diet-induced NASH in mice when administered individually. Furthermore, a combinatory therapy approach revealed that exercise and LTA exerted a synergistic effect on the alleviation of NASH phenotypes in mice. At the mechanistic level, exercise and LTA can synergistically increase the α-ketoglutarate (α-KG) level in hepatocytes to increase the transcription of *Nrf2* by inducing active DNA demethylation on its promoter. Our results suggest that, through promoting the α-KG/Nrf2 axis-mediated anti-oxidative pathway, the combination of LTA and exercise may provide an effective measure for the prevention and control of NASH.

2. Materials and methods

2.1 Animals

Animal experiments were approved by Shanghai University of Sport Animal Care and Use Committee (No. 102772022DW027). All studies involving animal experimentation followed the National Institute of Health guidelines on the care and use of animals. Male C57BL/6J mice were utilized in this study and subjected to the Gubra-Amylin NASH diet (GAN, D09100310, Research Diets) to induce hepatic fibrosis. These mice were housed in controlled environmental conditions ((23 ± 2) ℃, (50 ± 5)% humidity, and a 12-h light/dark cycle) and provided standard mouse feed and water *ad libitum* throughout the experimental period.

2.2 Treadmill training

Treadmill exercise regimen comprised a 3-day treadmill familiarization phase followed by an 8-week training program (6 days per week). During familiarization, mice ran on the treadmill at a speed of 10 m/min for 1 h per day. Subsequently, the treadmill training started at 12 m/min, with the running speed incrementally increasing by 2 m/min every 2 weeks. All mice underwent daily 1-h sessions on the treadmill. Continuous monitoring ensured that mice were consistently running and not resting, ensuring uniform exposure to the exercise regimen.

2.3 Primary hepatocytes isolation and cells culture

C57BL/6J mice (6–8 weeks old) were used in the experment. Primary hepatocytes were isolated by collagenase perfusion technique[32]. Liver tissue underwent perfusion and digestion[32]. After dissociation, the tissue was filtered, resulting in a cell suspension[32]. This suspension underwent centrifugation at 50 × *g* for 3 times to collect hepatocytes (cell pellets). Primary hepatocytes, along with HepG2 cells, were cultured in Dulbecco's Modified Eagle Media (DMEM) supplemented with 10% fetal bovine serum (FBS, Gibco, California, USA) at 37 ℃ in a 5% CO_2 environment (Thermo Fisher

Scientific, Massachusetts, USA). LTA (CAS: 3081-61-6,) was purchased from Shandong Topscience Biotech Co., Ltd. (T2800) and dissolved in saline.

2.4 Lipid analysis

To elucidate the hepatic steatosis and apoptosis effects of LTA, primary hepatocytes were seeded in 6-well plates. After cell adhesion, 0.6 mmol/L mixture of free fatty acids (FFAs) was added to the medium for 36 h with or without LTA (at a final molar ratio of 2:1 with oleic acid (OA) and palmitate (PA); Sangon Biotech, Shanghai, China)[32]. Following that, the cells underwent fixation with 4% paraformaldehyde for a specified duration and subsequent staining with Nile red and Hoechst for a designated period to observe and analyze intracellular lipid accumulation[32]. According to the manufacturer's instructions, the TG, total cholesterol (TC) content was measured using kits from Applygen Co., Ltd. (#E1003 and #E1005, respectively; Beijing, China)[32].

2.5 Biochemical analysis

The blood samples were collected using eyeballs plexus and centrifuged at 3 000 r/min for 10 min, then serum was collected for biochemical analysis[29]. Levels of serum ALT, and AST were measured using the kits from Applygen Co., Ltd. (#E2021 and #E2023, respectively; Beijing, China) according to the manufacturer's instructions[29]. Malondialdehyde (MDA) level was measured by using the kit from Beyotime (S0131M; Shanghai, China). Hydroxyproline level was measured by using the kit from Nanjing Bioengineering Institute (A030-2-1; Nanjing, China). Insulin level was measured using the kit from Mercodia (10-1247-01; Uppsala, Sweden).

2.6 RNA interference

RNAiMAX (#13778-100, Invitrogen; California, USA) was used for the transfection according to the manufacturer's protocol. The nonspecific small interfering RNA (siRNA) control (siNC) served as the negative control in the experimental setup[33-34]. The target sequences for successful siRNAs (5′ to 3′) were as follows (Genepharma, China): *siNrf2-1* (mouse), GCAGAATTATAGCCAAAGCTA; *siNrf2-2* (mouse), CCCGAATTACAGTGTCTTAAT; *siNrf2-1* (human), GCTCCTACT GTGATGTGAAAT; *siNrf2-2* (human) CCGGCATTTCACTA AACACAA; *siNC*, TTCTCCGAACGTGTCACGT. *siNrf2-1* and *siNrf2-2* target different sites of the human or mouse gene of *Nrf2*.

2.7 Hematoxylin-eosin (H&E), Sirius red and F4/80 staining

The tissues were subjected to fixation in 4% paraformaldehyde, followed by embedding in paraffin and subsequent sectioning. H&E, Sirius red and F4/80 staining were then performed. The procedure follows the previously established protocol[33]. For analyses related to Sirius red staining and F4/80 immunofluorescence, computer image analysis was employed using ImageJ from the National Institutes of Health (NIH). The quantification involved determining the percentage of stained area relative to the total field of view. Consistent threshold settings were applied across all analyses for accuracy and comparability[35].

2.8 Cell viability assay

Cell viability was assessed utilizing the cell counting kit-8 (CCK-8) following the guidelines provided by the manufacturer (MedChemExpress, New Jersey, USA).

2.9 RNA extraction and reverse transcription-quantitative polymerase chain reaction (RT-qPCR)

For RNA extraction from both cells and tissues, Trizol reagent (Invitrogen) was employed following the manufacturer's guidelines. Complementary DNA (cDNA) synthesis was achieved from total RNA using a reverse transcription kit (Beyotime, Shanghai, China)[36]. Amplification of cDNAs was performed with Power SYBR Green PCR Master Mix (Beyotime, Shanghai, China), using 18S rRNA or *36b4* as an endogenous control[37]. The qPCR procedure was executed in triplicate and repeated a minimum of 3 times[38]. Table S1 provides primer information for RT-qPCR.

2.10 Immunoblotting analysis

Cells and tissues were collected and processed for immunoblotting following a previously outlined procedure. Briefly, lysates were separated on SDS-PAGE gel, and immunoblotting was conducted using primary antibodies specific to collagen 1a1 (A1352; ABclonal, Wuhan, China), cleaved Caspase-3, Nrf2 (16396-1-AP, Proteintech, Wuhan, China), HO-1 (10701-1-AP, Proteintech, Wuhan, China), SOD2 (24127-1-AP; Proteintech Wuhan, China), *β*-tubulin (MA5-16308; Thermo Fisher Massachusetts, USA), and GAPDH (D16H11; CST, Boston, USA). ImageJ was employed for quantification, with target protein values normalized to the internal control protein on the same membrane[39].

2.11 Determination of reactive oxygen species (ROS)

Total cellular ROS levels were assessed using 2,7-dichlorofluorescin diacetate (DCFH-DA) probe from Applygen (C1300-1; Beijing, China). For measuring ROS in mice livers, 20 mg liver tissues were homogenized in 500 μL of PBS. Subsequently, the tissue homogenate was incubated with 10 μmol/L DCFH-DA at 37 °C for 30 min. Following this, the homogenate underwent centrifugation at 500 × *g* for 5 min, followed by 2 washes with PBS. Fluorescence measurements were then taken[37].

2.12 Ten-eleven translocation hydroxylase (TETs) activity assay

Primary hepatocytes and nuclei from liver tissues were isolated utilizing Nuclear and Cytoplasmic Extraction Reagents (P0027; Beyotime, Beijing, China). The evaluation of TETs activity was conducted employing the kit (ab156913, Fluorometric; Abcam, Cambridge, UK), in accordance with the protocols provided by the manufacturer.

2.13 Chromatin immunoprecipitation (ChIP)

ChIP was performed as described previously[33,40]. Cell cross-linking: mice primary hepatocytes were cross-linked in 1%

formaldehyde for 10 min at room temperature. Termination of cross-linking was done by incubating the cells with 125 mmol/L glycine. Cell lysis: after cross-linking, cells were washed twice with ice-cold PBS, then cells were resuspended in 500 μL of lysis buffer (containing 50 mmol/L Tris-HCl (pH 8.0), 1% SDS, 10 mmol/L EDTA, and protease inhibitors). Sonication: samples were sonicated to shear the chromatin, resulting in DNA fragments with an average length ranging between 200 and 800 bp. Centrifugation: the samples were centrifuged at 12 000 × *g* at 4 ℃ for 5 min. Dilution: supernatants were diluted 10-fold in ChIP dilution buffer containing 20 mmol/L Tris-HCl (pH 8.0), 150 mmol/L NaCl, 2 mmol/L EDTA, 1% Triton X-100, and complete protease inhibitor tablets. Pre-clearing: each sample was precleared using ChIP grade protein A/G magnetic beads for 1 h at 4 ℃ . Immunoprecipitation: immunoprecipitation was performed using specific antibodies against HO-1 and SOD2, as well as a control IgG. Antibodies: anti-HO-1 (10701-1-AP), anti-SOD2 (24127-1-AP; Proteintech), and control IgG (b46540; Abcam). Elution: immunoprecipitated samples were eluted and reverse cross-linked by incubation overnight at 65 ℃ in elution buffer. DNA extraction: genomic DNA was extracted using a PCR purification kit (Qiagen). qPCR: purified DNA was subjected to qPCR using primers specific to the promoters of the indicated genes[41].

2.14 Hydroxymethylated and methylated DNA immunoprecipitation (MedIP)

MedIP was performed as described previously[33]. MedIP steps include genomic DNA extraction, DNA ultrasound, DNA purification, denaturation, and immunoprecipitation (IP), washing and digestion, quantification, and data analysis. Reagent information used is as follows: Blood/Cell/Tissue genomic DNA extraction kit (DP304; Tiangen, Beijing, China), 5-hmc (A4001; Zymo Research), 5-mc antibody (A3001; Zymo Research), pierce magnetic protein A/G (88802; Thermo Scientific), and 36b4 promoter as a negative control.

2.15 Statistical analysis

The presented data represent the means ± standard deviation (SD) derived from a minimum of 3 distinct biological replicates. Details of the statistical analyses are provided in the legends of individual figures, and statistical significance is denoted by $P < 0.05$. The statistical analysis was conducted using GraphPad Prism (Version 9). The representing mouse model was created using Med Peer.

3. Results

3.1 Construction of the Gubra-amylin NASH (GAN) diet-induced NASH model in mice

Excessive intake of diets high in saturated fats, fructose, and cholesterol is widely acknowledged as a major factor contributing to the onset and advancement of NAFLD/NASH[42-44]. GAN diet-induced obesity in mice serves as a clinically translatable model, mimicking key aspects of disease etiology and NASH characteristics[44]. Notably, the GAN diet, abundant in these nutrient components, induces obesity and consistently leads to biopsy-confirmed NASH and fibrosis in C57BL/6 mice[44]. In our research, we conducted NASH phenotyping in male C57BL/6J mice subjected to the GAN diet. The mice were randomly divided into 2 groups, one group fed a 25-week GAN diet and the other with a 25-week normal control diet (NCD) as a comparative control (Fig. 1A). Comparative analysis revealed that mice on the GAN diet exhibited significantly higher body weight gain and increased liver weight compared to those in the NCD group (Figs. 1B-D). Furthermore, compared to the control group, hepatic TG (Fig. 1E) and hepatic TC (Fig. 1F) levels were notably elevated in the GAN group. Insulin resistance, recognized as a pivotal factor in NASH and associated metabolic syndrome, was assessed in mice from both groups. The NASH mice displayed significantly higher fasting blood glucose levels (Fig. 1G) and fasting insulin levels (Fig. 1H) compared to the control mice. The homeostasis model assessment-insulin resistance (HOMA-IR) index was also notably increased in the NASH group (Fig. 1I), indicating the development of insulin resistance following 25 weeks of GAN diet feeding. Furthermore, liver sections were subjected to H&E staining, Sirius red staining, and F4/80 staining. H&E staining revealed severe steatosis in the livers of mice on the 25-week GAN diet, characterized by enlarged lipid droplets and a significant increase in lipid accumulation (Fig. 1J). This comprehensive analysis provides insights into the impact of the GAN diet on obesity, NASH development, and associated metabolic changes in mice. Sirius red staining (Figs. 1J and K) of liver indicated the development of pericellular liver fibrosis in GAN diet-fed mice, and the abundance of F4/80-positive macrophages was increased (Figs. 1J and L). In comparison to mice consuming the NCD, those subjected to the GAN diet displayed a notable increase in serum ALT (Fig. 1M) and AST (Fig. 1N). Consistent with the F4/80 and Sirius red staining results, the expression levels of inflammation and fibrosis genes were markedly induced in GAN diet-fed mice (Fig. 1O). Furthermore, immunoblotting analysis of liver lysates revealed increased protein levels of collagen 1a1 and cleaved Caspase-3 in response to GAN diet feeding (Figs. 1P and Q).

In summary, these findings collectively demonstrate that GAN diet feeding reproduces critical pathological events associated with NASH in mice. These events encompass hepatic steatosis, inflammation, fibrosis, and apoptosis within the context of obesity. Importantly, after 25 weeks of intervention, these histological features were fully established.

3.2 Synergistic effects of exercise and LTA on alleviating obesity-related metabolic disorders in NASH mice

Role of LTA and exercise in alleviating NASH was investigated in the GAN diet-fed mouse model. Because NASH is usually associated with obesity and metabolic disorders, the effects of LTA and exercise on alleviating the above phenotypes were examined first. Our previous research confirmed that aerobic exercise is effective in reducing the accumulation of liver fat[37]. Therefore, we used moderate-intensity treadmill training as an exercise intervention strategy. GAN diet-fed mice were randomly divided into the following 4 groups: Saline/Sed (saline + sedentary life style), Saline/Ex (saline + exercise training), LTA/Sed (LTA + sedentary life style), and LTA/Ex (LTA + exercise training), which is shown in Fig. 2A. LTA was administered daily for 8 weeks as an oral supplement by

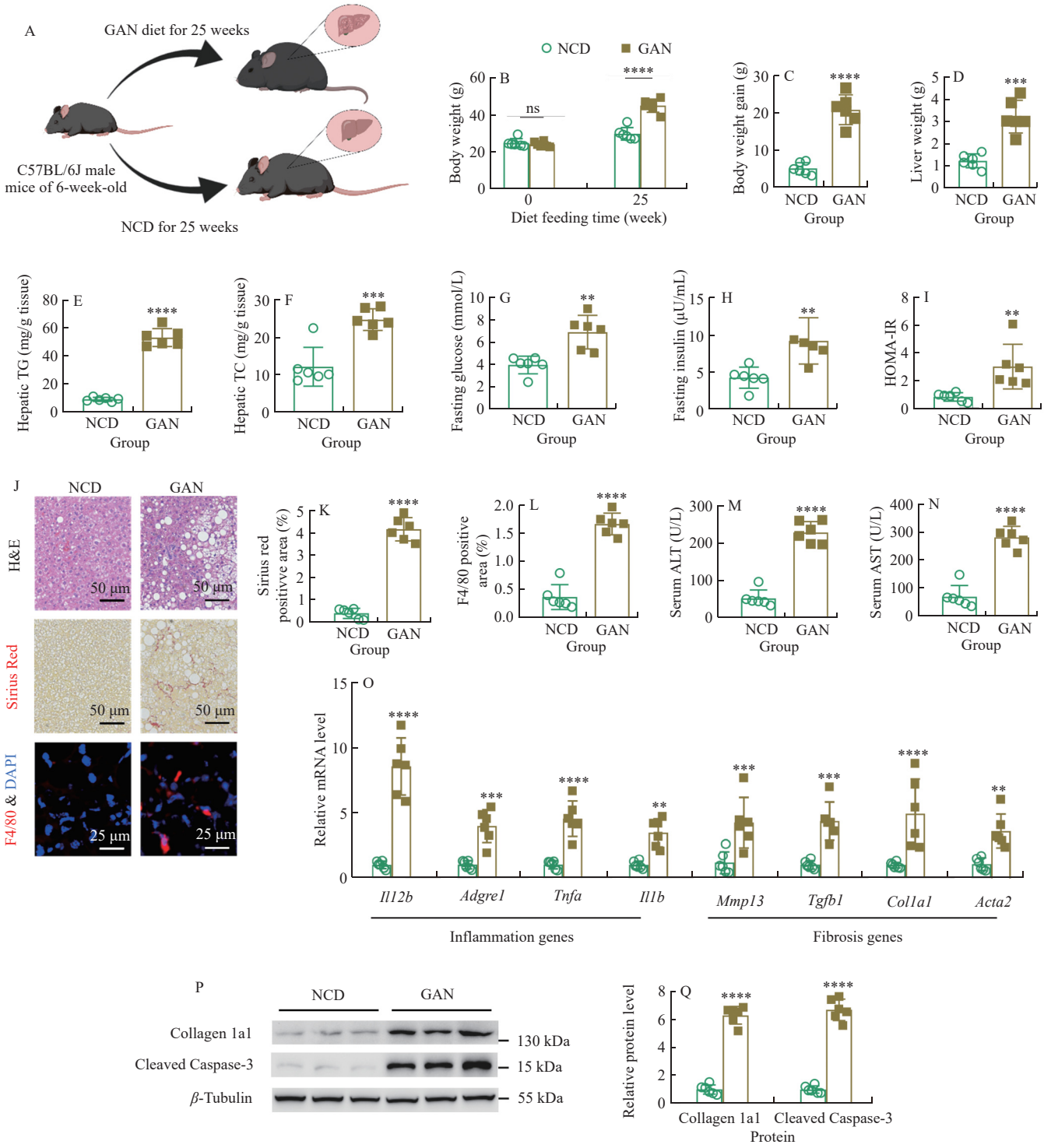

Fig. 1 Construction of the GAN diet-induced NASH model in mice. (A) Experimental setup. The representing mouse model was created using Med Peer. (B) Body weight in mice. (C) Body weight gain in mice. (D) Liver weight in mice. (E) Hepatic TG level of the mice. (F) Hepatic TC level of the mice. (G) Fasting blood glucose of the mice. (H) Fasting insulin levels of the mice. (I) HOMA-IR of the mice. (J) Representative images of H&E staining, Sirius red staining and F4/80 fluorescence analysis of mice liver sections. Scale bars, 50 μm for H&E staining and Sirius staining, and 25 μm for F4/80 fluorescence. (K and L) Sirius red staining and F4/80 fluorescence analysis and (J) quantification results was done by ImageJ. (M) Serum ALT levels in mice. (N) Serum AST levels in mice. (O) mRNA levels of the indicated genes in mice livers were determined by using RT-qPCR. Data normalized to the NCD group. (P) Immunoblotting analysis of the protein levels in mice livers by using the indicated antibodies. *β*-Tubulin serves as an internal control. (Q) Quantification of immunoblotting results was done by ImageJ ($n = 6$). Unpaired two-tailed *t*-tests were performed. All data show the means ± SD, $n = 6$. $^{**}P < 0.01$, $^{***}P < 0.001$, $^{****}P < 0.000\,1$, ns. not significant, comparing to NCD group.

gastric needle at a dose level of 300 mg/kg body weight. The treadmill training program was illustrated in Fig. 2B. Compared with the Saline/Sed mice, Saline/Ex mice or LTA/Sed mice had significantly lower body weight, after 8-week intervention (Fig. 2C). Saline/Ex group exhibited significant lower body weight gain than the Saline/Sed, and the LTA/Sed group had a lower trend of body weight gain (Fig. 2D). Exercise or LTA intervention led to significantly lower liver weights compared to the control intervention (Fig. 2E). In addition, hepatic TG (Fig. 2F), hepatic TC (Fig. 2G) and serum TC (Fig. 2H) in Saline/Ex and LTA/Sed groups were significantly lower compared to the Saline/Sed group. Furthermore, we observed that both exercise and LTA treatment improved insulin resistance in mice, as indicated by significantly lower fasting blood glucose (Fig. 2I), fasting blood insulin level (Fig. 2J) and HOMA-IR index (Fig. 2K) in

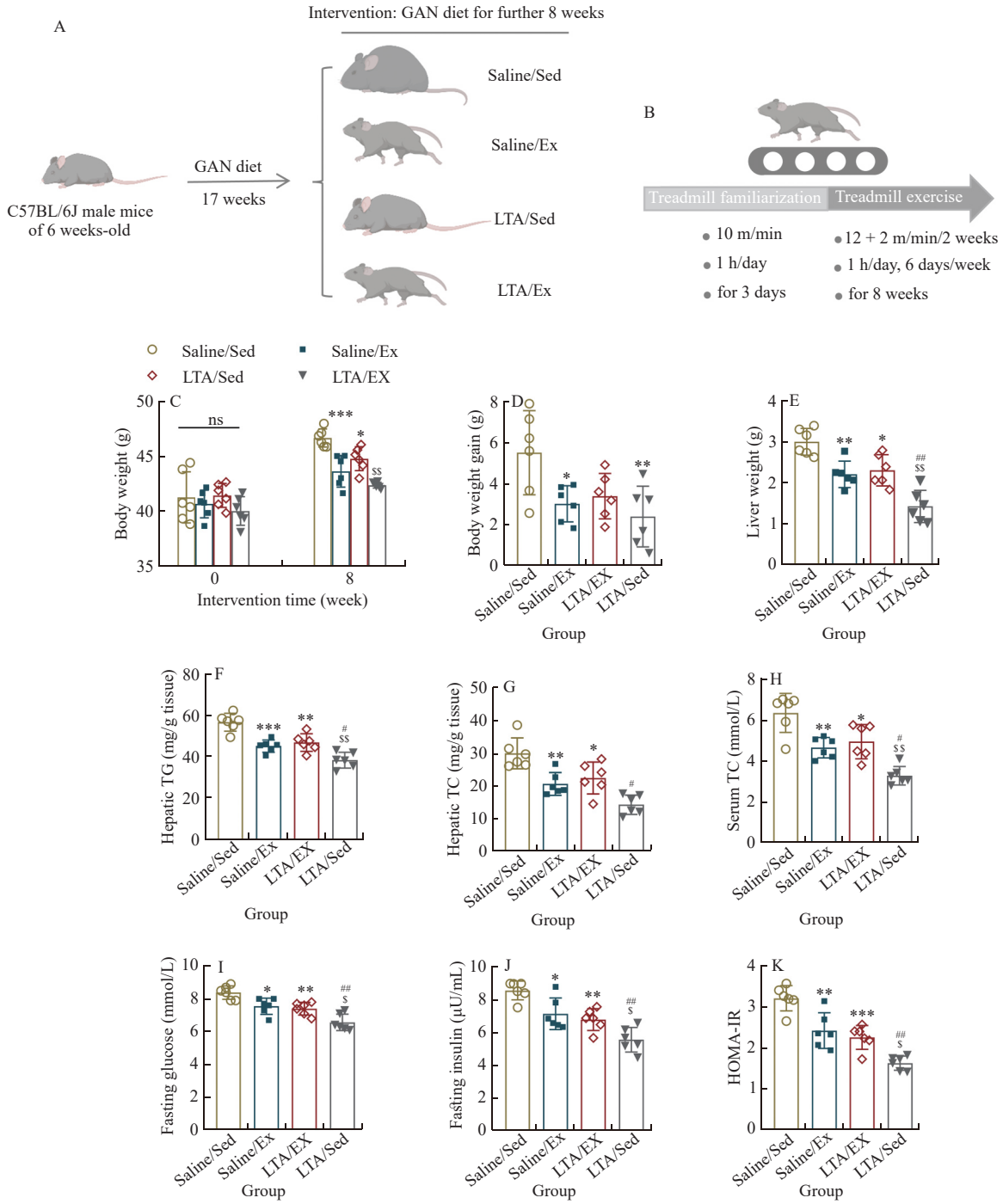

Fig. 2 Synergistic effects of exercise and LTA on alleviating obesity-related metabolic disorders in NASH mice. (A) Experimental setup. (B) The treadmill exercise program. (C) Mice body weight. (D) Body weight gain in mice. (E) Mice liver weight. (F) Hepatic TG levels. (G) Hepatic TC levels. (H) Serum TC levels. (I) Fasting blood glucose of the mice. (J) Fasting insulin levels of the mice. (K) HOMA-IR of mice. Two-way analysis of variance plus Tukey's post hoc tests were performed. All data show the means ± SD, $n = 6$. $^{*}P < 0.05$, $^{**}P < 0.01$, $^{***}P < 0.001$, comparing to Saline/Sed group; $^{\#}P < 0.05$, $^{\#\#}P < 0.01$, comparing to the Saline/Ex group; $^{\$}P < 0.05$, $^{\$\$}P < 0.01$, comparing to LTA/Sed group; ns. not significant.

the Saline/Ex and LTA/Sed groups than in the Saline/Sed group. Importantly, as shown in Figs. 2C-K, it was found that the combination of exercise and LTA treatment (LTA/Ex) could more efficiently improve the above parameters than the single exercise intervention (Saline/Ex) and the single LTA treatment (LTA/Sed). The above data demonstrate that both exercise and LTA can improve obesity-related metabolic disorders in NASH mice, and they can exert synergistic effects on combating the above disorders.

3.3 Exercise and LTA synergize to ameliorate the NASH phenotypes in mice

Roles of exercise and LTA intervention in NASH were then investigated. The immunohistochemical and immunofluorescence staining of the liver is shown in Fig. 3A. Compared to the Saline/Sed group, both exercise and LTA single intervention significantly reduced hepatic steatosis. Importantly, the combination of exercise and LTA

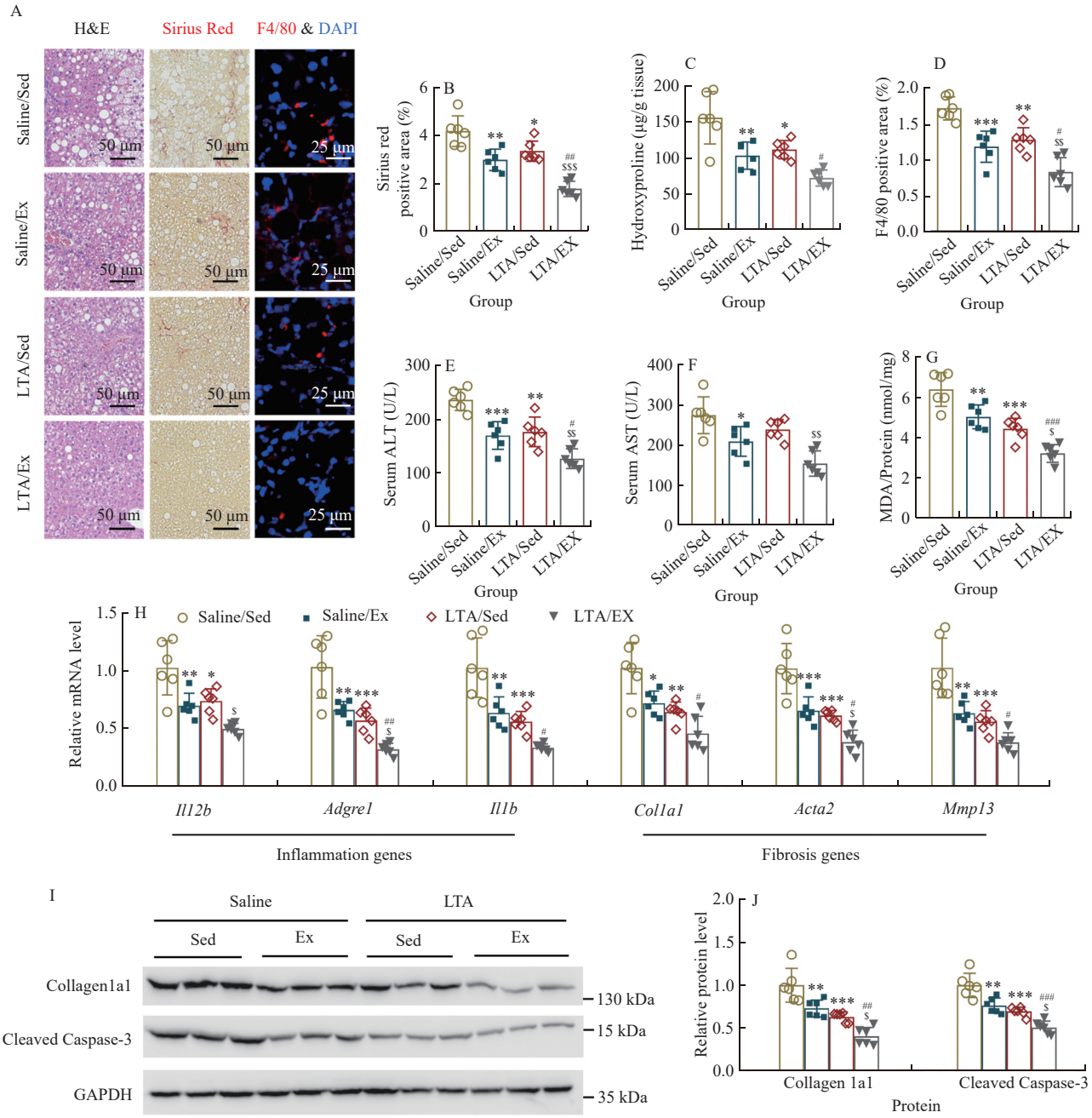

Fig. 3 Exercise and LTA synergize to ameliorate the NASH phenotypes in mice. (A) Representative images of H&E staining, Sirius staining and F4/80 fluorescence analysis of liver sections. Scale bars, 50 μm for H&E staining and Sirius Red staining, and 25 μm for F4/80 fluorescence. (B) Quantification of Sirius red staining analysis. (C) Hydroxyproline level in mice livers. (D) Quantification of F4/80 fluorescence staining analysis. (E) Serum ALT level in mice. (F) Serum AST level in mice. (G) Hepatic MDA level of mice livers. (H) mRNA levels of the indicated genes in mice livers. Data normalized to the Saline/Sed group. (I) Immunoblotting analysis of the protein levels in mice livers. GAPDH serves as an internal control. (J) Quantification of immunoblotting results. Two-way analysis of variance plus Tukey's post hoc tests were performed. All data show the means ± SD, $n = 6$. $^{*}P < 0.05$, $^{**}P < 0.01$, $^{***}P < 0.001$, comparing to Saline/Sed group; $^{\#}P < 0.05$, $^{\#\#}P < 0.01$, $^{\#\#\#}P < 0.001$, comparing to the Saline/Ex group; $^{\$}P < 0.05$, $^{\$\$}P < 0.01$, $^{\$\$\$}P < 0.001$, comparing to LTA/Sed group.

intervention led to a more pronounced reduction in hepatic steatosis (Fig. 3A). Biochemical analysis of intrahepatic lipids (Figs. 2F and G) substantiated these results and revealed that the significant reduction in hepatic TG and hepatic TC contributed to the reduction in hepatic steatosis by exercise and LTA. Besides, the combination of exercise and LTA intervention more efficiently reduced hepatic TG and hepatic TC levels (Figs. 2F and G), thereby more efficiently alleviating hepatic steatosis. In comparison to the Saline/Sed group, both Saline/Ex mice and those receiving LTA showed reduced collagen deposition in the liver, as indicated by Sirius red staining, computerized analysis of histological slices for collagen deposition, and measurements of liver hydroxyproline content (Figs. 3A-C). Both exercise and LTA intervention independently inhibited liver fibrosis, and their combination further attenuated this condition (Figs. 3A-C). Additionally, both exercise and LTA led to a decrease in F4/80-positive macrophages, with their combination demonstrating greater efficacy in reducing this parameter (Figs. 3A and D). Then we examined markers of liver damage. Serum levels of ALT and AST were decreased in Saline/Ex group and LTA/Sed group following GAN diet feeding, which was further reduced after the combination of exercise and LTA intervention (Figs. 3E and F). MDA level, the marker of oxidative stress, was significantly reduced after exercise and LTA interventions, and their combined intervention yielded better effects (Fig. 3G). Additionally, the mRNA expression of genes related to liver fibrosis and inflammation were downregulated the Saline/Ex group and the LTA/Sed group under GAN diet-fed conditions, and the combination of the 2 treatments more efficiently inhibited the expression of these genes (Fig. 3H). Consistently, following GAN diet feeding, the protein levels of collagen 1a1 (fibrosis marker) and cleaved Caspase-3 (apoptosis marker) were decreased after exercise or LTA treatment, and combinatory intervention further inhibited the expression of the 2 proteins (Figs. 3I and J). The above data indicate that exercise and LTA intervention blunted GAN diet-induced hepatic steatosis, hepatic inflammation and fibrosis in mice, and additive effects were observed upon the combination of exercise and LTA intervention. Therefore, our results demonstrate that exercise and LTA can ameliorate the phenotypes of NASH in mice in a synergistic manner.

3.4 Exercise and LTA synergistically up-regulate Nrf2 via α-KG/TETs/DNA demethylation axis to inhibit oxidative stress in the liver

Nrf2 is reported to play an important role in limiting the progression of NASH, which could be ascribed to the upregulation of anti-oxidative genes, such as HO-1 and SOD2[45-46]. To verify the role of Nrf2 in LTA and exercise-mediated alleviation of diet-induced NASH, we examined the expression of Nrf2 and its downstream target genes in mice livers after LTA and exercise intervention. In mice livers, LTA significantly increased the mRNA expression levels of *Nfe2l2*, *Homx1* and *Sod2* (Fig. 4A) and promoted the expression levels of anti-oxidative stress proteins, Nrf2 and HO-1 (Figs. 4B and C), in GAN diet-fed mice livers. Interestingly, exercise can also enhance the expression of the above anti-oxidative genes and proteins, and the combination of exercise and LTA exhibited additive effects on promoting their expression (Figs. 4A-C). These data indicate that exercise and LTA may inhibit hepatic oxidative stress to protect against NASH diet-induced liver injury, through upregulating the expression of Nrf2 and its downstream target genes in a synergistic manner. As the expression of Nrf2 was upregulated by exercise and LTA, the underlying mechanism of how Nrf2 expression was regulated during these processes was then investigated. DNA methylation is a complex regulatory process that is important for regulating genes expression. We then investigated the levels of DNA methylation (5-mc) and hydroxymethylation (5-hmc) across the regions of the *Nrf2* promoter in mice livers. As shown in Figs. 4D and E, exercise and LTA led to decrease of 5-mc level and the elevation of 5-hmc level significantly on *Nrf2* gene promoter of mice livers, and the combination of exercise and LTA intervention led to more efficient role. In line with this, both exercise and LTA was able to increase the enzyme activity of TETs, the DNA demethylase, and their combination exhibited synergistic effects on enhancing TETs enzyme activity (Fig. 4F). α-KG is a crucial intermediate of the Krebs cycle. It has previously been reported that α-KG can function as a co-factor of TETs DNA demethylase to promote DNA demethylation, thereby increasing genes expression[47]. It is reported that LTA could increase the cellular α-KG level in adipocytes to promote the expression of thermogenic genes[48]. Studies were then performed to investigate whether exercise or LTA could facilitate the DNA demethylation on *Nrf2* gene promoter through up-regulating of the cellular level of α-KG in hepatocytes. It was shown that the level of hepatic α-KG was significantly increased by both exercise and LTA (Fig. 4G). Combination of exercise and LTA intervention had an additive effect on the elevation of hepatic α-KG level (Fig. 4G). These results suggest that LTA and exercise may enhance TETs activity by increasing the level of α-KG in mice livers. Overall, our findings suggest that, in NASH mice livers, exercise and LTA promote DNA demethylation of the *Nrf2* gene promoter, facilitating *Nrf2* expression by upregulating the hepatic level of α-KG.

3.5 LTA alleviates steatosis, oxidative stress and apoptosis in free fatty acids-treated hepatocytes

To elucidate the effects of LTA on hepatic steatosis and apoptosis, an *in vivo* model was established by treating mice primary hepatocytes or HepG2 cells with FFAs according to previous studies[49-50]. As described previously[51], we used the mixture of OA and PA (2:1 of molar ratios) to establish the cellular model of hepatic steatosis (Fig. S1). Mice primary hepatocytes or HepG2 cells were pretreated with or without LTA for 8 h, and then were subjected to a 36-h treatment of FFAs in the presence or absence of LTA. After 36 h of treatment, cells were harvested for analyses; PBS was used as the vehicle control (vehicle group) (Fig. 5A). Intracellular levels of TG in mice primary hepatocytes (Fig. 5B) and HepG2 cells (Fig. S2A) were remarkably decreased by LTA treatment compared with the vehicle group (without LTA treatment). LTA demonstrated a dose-dependent inhibition of the buildup of intracellular lipid accumulation in primary hepatocytes (Fig. 5B). Nile red staining in primary hepatocytes (Fig. 5C) and HepG2 cells (Fig. S2B) revealed that lipid droplets amount was significantly decreased in LTA group. These results above indicate that LTA decreased the TG content in hepatocytes to attenuate hepatic steatosis. Moreover, the level of reactive oxygen species (ROS) was remarkably decreased by LTA in mice primary hepatocyte and HepG2 cells (Figs. 5D and S2C). In line with this, the level of hepatocyte MDA was down-regulated in LTA-treated

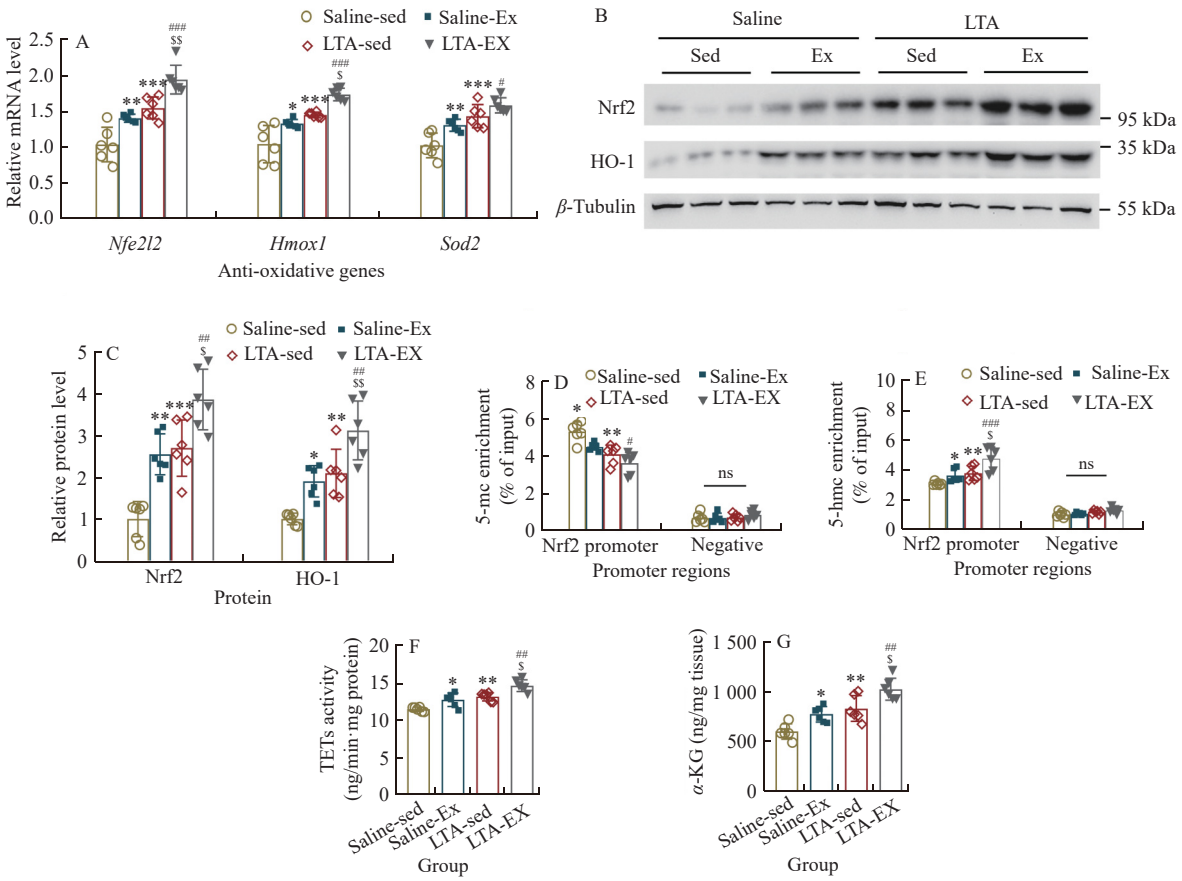

Fig. 4 Exercise and LTA synergistically up-regulate Nrf2 *via* α-KG/TETs/DNA demethylation axis to inhibit oxidative stress in the liver. (A) mRNA levels of the indicated genes in mice livers were determined by using RT-qPCR. Data normalized to the Saline/Sed group. (B) Immunoblotting analysis of the protein levels in mice livers by using the indicated antibodies. β-tubulin serves as an internal control. (C) Quantification of immunoblotting results done by ImageJ. The enrichment level of (D) hepatic 5-mc and (E) 5-hmc on the Nrf2 promoter of mice. (F) The activity of hepatic TETs of mice was measured and shown. (G) Hepatic α-KG of mice was measured and shown. Two-way analysis of variance plus Tukey's post hoc tests were performed in (A and C-G). All data show the means ± SD, $n = 6$. $^{*}P < 0.05$, $^{**}P < 0.01$, $^{***}P < 0.001$, comparing to Saline/Sed group; $^{\#}P < 0.05$, $^{\#\#}P < 0.01$, $^{\#\#\#}P < 0.001$, comparing to the Saline/Ex group; $^{\$}P < 0.05$, $^{\$\$}P < 0.01$, comparing to LTA/Sed group; ns. not significant.

primary hepatocyte and HepG2 cells (Fig. 5E and S2D), which indicates that LTA inhibits FFA-induced hepatocyte oxidative stress. Immunoblotting showed that LTA inhibited apoptosis (Figs. 5F and G), and CCK-8 assay also revealed a decrease in cell death after LTA intervention (Figs. 5H and S2E). In summary, *in vivo* experiments demonstrate that FFA induces hepatocyte lipid accumulation, leading to increased ROS production and hepatocyte oxidative stress, ultimately leading to hepatocytes apoptosis. Moreover, LTA can attenuate FFA-induced hepatic steatosis, oxidative stress and apoptosis.

3.6 Knocking down Nrf2 impairs LTA-mediated protective effects against hepatocytes oxidative stress and injury

As mentioned above, LTA can inhibit oxidative stress and cellular injury in mice liver. To verify the role of Nrf2 in LTA-mediated alleviation of hepatocytes injury, we examined the expression of Nrf2 and its downstream target genes in hepatocytes after LTA intervention. In mice primary hepatocytes, LTA increased the expression levels of *Nfe2l2*, *Homx1* and *Sod2* genes compared with the vehicle group (Fig. 6A). Similar results were obtained in HepG2 cells (Fig. S2F). Consistently, immunoblotting revealed that the protein levels of Nrf2 and HO-1 were increased by LTA treatment (Figs. 6B and C). Furthermore, ChIP was performed and it was found that LTA promoted the binding of *Nrf2* to the gene promoters of *HO-1* and *SOD2*, indicating that LTA enhanced the transactivation of *Nrf2* target genes (Figs. 6D and E). The above experiments reveal that LTA can promote the expression of *Nrf2* and other anti-oxidative genes in hepatocytes. These results prompt us to explore the role of Nrf2 in LTA-mediated protection against hepatocellular injury. Mice primary hepatocytes were transfected with the indicated siRNAs. After 12 h, cells were then treated as described in Fig. 5A. When we used siRNA to knock down Nrf2 in primary hepatocytes and HepG2 cells, it was found that the effects of LTA on the alleviation of FFAs-induced hepatocyte lipid accumulation and damage were significantly attenuated (Figs. 6F-M and Fig S3). Specifically, when comparing the siNC group, the knockdown of *Nrf2* (siNrf2 group) led to lower anti-oxidative genes and proteins expression and promoted the expression of apoptosis-related protein cleaved Caspase-3 in mice primary hepatocytes (Figs. 6F-H). Similar results were obtained in HepG2 cells (Figs. S3A-C). More importantly, LTA-mediated upregulation of anti-oxidative gene expression, and decrease of cleaved Caspase-3 level, were

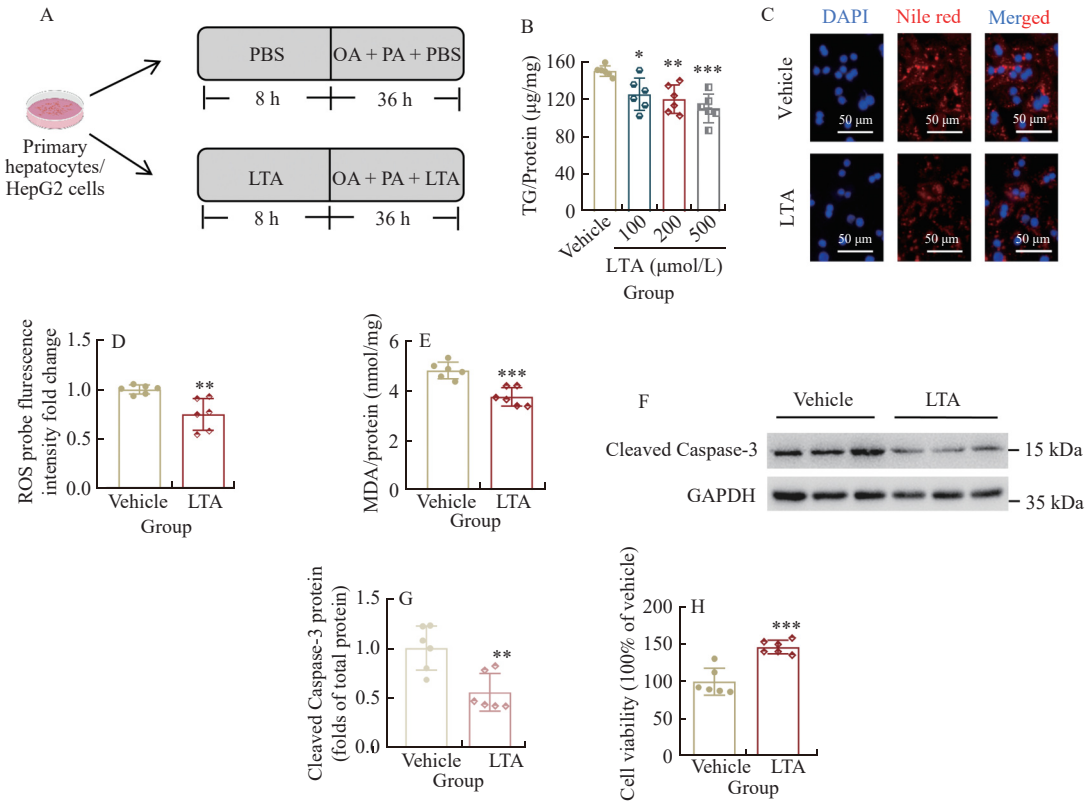

Fig. 5 LTA alleviates steatosis, oxidative stress and apoptosis in free fatty acids (FFAs)-treated hepatocytes. (A) Experimental setup. (B) TG level of primary hepatocytes. (C) Representative picture of Nile red and Hoechst staining of primary hepatocyte. Scale bars, 50 μm. (D) Cellular ROS levels; (E) Level of MDA in primary hepatocytes; (F) Immunoblotting analysis of the protein levels in primary hepatocytes (GAPDH serves as an internal control); (G) Quantification of immunoblotting results; (H) Cell viability of primary hepatocytes. 200 μmol/L LTA was used. One-way analysis of variance plus Tukey's post hoc tests was performed in (B); unpaired two-tailed *t*-tests were performed in (D, E, G, H). All data show the means ± SD, $n = 6$. $^{*}P < 0.05$, $^{**}P < 0.01$, $^{***}P < 0.001$, comparing to vehicle group.

significantly attenuated upon the knockdown of *Nrf2* (Figs. 6F-H and S3A-C). Besides, more lipid accumulation and higher cellular TG levels were observed when knocking down *Nrf2* (Figs. 6I-J and S3D-E). LTA-mediated inhibition of cellular lipid accumulation is significantly weakened when *Nrf2* was knocked down. Elevated cellular ROS levels were observed in cells with *Nrf2* knockdown, indicating the deficiency of Nrf2 increased oxidative stress (Figs. 6K and S3F). In the context of siNrf2, the ability of LTA to decrease ROS levels was significantly weakened, underscoring the crucial role of Nrf2 in LTA-mediated inhibition of ROS accumulation. Correspondingly, *Nrf2* knockdown led to heightened cellular MDA levels, and the effectiveness of LTA in inhibiting MDA accumulation was

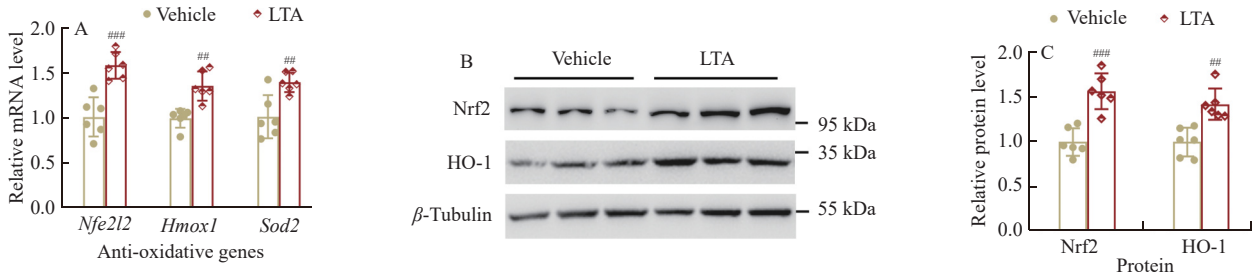

Fig. 6 Knocking down *Nrf2* impairs LTA-mediated protective effects against hepatocytes oxidative stress and injury. (A) mRNA levels of the indicated genes in mice primary hepatocytes were determined by using RT-qPCR. Data normalized to the vehicle group. (B) Immunoblotting analysis of the protein levels in primary hepatocytes by using the indicated antibodies. *β*-Tubulin serves as an internal control. (C) Quantification of immunoblotting results done by ImageJ. (D and E) Binding of *Nrf2* to the promoters of *HO-1* and *SOD2* was measured by ChIP. (F) The mRNA levels of the indicated genes in primary hepatocytes were determined by using RT-qPCR. Data normalized to the siNC/Vehicle group. (G) Immunoblotting analysis of the protein levels in primary hepatocytes using the indicated antibodies. *β*-Tubulin serves as an internal control. (H) Quantification of immunoblotting results done by using ImageJ. (I) Representative picture of Nile red and Hoechst staining of primary hepatocyte. Scale bars, 50 μm. (J) TG in primary hepatocytes. (K) Cellular ROS level. (L) Level of MDA in primary hepatocytes. (M) Cell viability of primary hepatocytes. 200 μmol/L LTA was used in the experiments. Unpaired two-tailed *t*-tests were performed in (A and C). Two-way analysis of variance plus Tukey's post hoc tests were performed (D-F, H and J-M). All data show the means ± SD, $n = 6$. $^{\#\#}P < 0.01$, $^{\#\#\#}P < 0.001$, comparing to vehicle group. $^{\$\$\$}P < 0.001$, $^{*}P < 0.05$, $^{**}P < 0.01$, $^{***}P < 0.001$, comparing siNC/Vehicle group. ns. no significant difference.

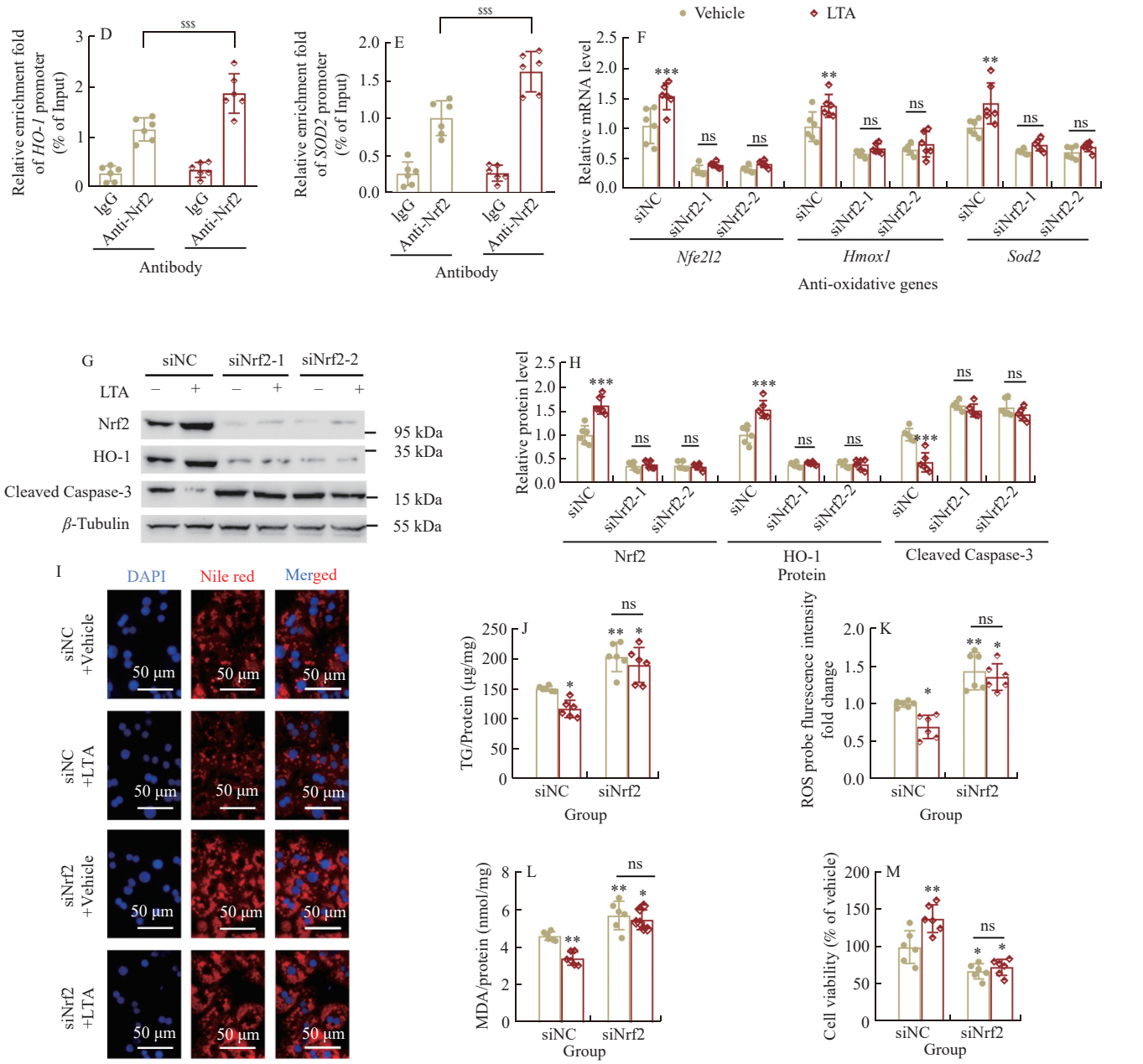

Fig. 6 (*Continued*)

significantly reduced upon *Nrf2* knockdown (Figs. 6L and S3G). Consistently, it was found that knockdown of *Nrf2* inhibited cell survival and the effects of LTA on the enhancement of cell survival were significantly blunted by *Nrf2* knockdown (Fig. 6M and S3H). These findings collectively underscore the important role of Nrf2 in LTA-mediated protection against hepatocellular injury, including steatosis, oxidative stress and apoptosis.

3.7 LTA increases the cellular content of α-KG and decreases the DNA methylation level of Nrf2 promoter in hepatocytes

Consistent with *in vitro* experiments (Fig. 4G), the α-KG concentration was determined and showed a dose-dependent elevation by LTA treatment in mice primary hepatocytes (Fig. 7A). Consistently, LTA treatment significantly enhanced TETs activity in mice primary hepatocytes (Fig. 7B). As depicted in Figs. 7C and D, the levels of 5-mc on the three regions of the *Nrf2* gene promoter was reduced and that of 5-hmc was enhanced significantly by LTA. Furthermore, inhibition of TETs enzyme activity weakened LTA impact on elevating mRNA and protein expression levels of Nrf2 (Figs. 7E-G). These results underscore the pivotal role of DNA demethylation on the *Nrf2* gene promoter in mediating LTA-induced up-regulation of Nrf2 expression. In addition, studies were performed to investigate whether α-KG is involved in the above-mentioned Nrf2 epigenetic changes caused by LTA. Therefore, we pretreated primary hepatocytes with α-KG (25 μmol/L) for 24 h, followed by FFAs challenge for another 36 h. As shown in Figs. 7H-J, α-KG significantly increased the mRNA and

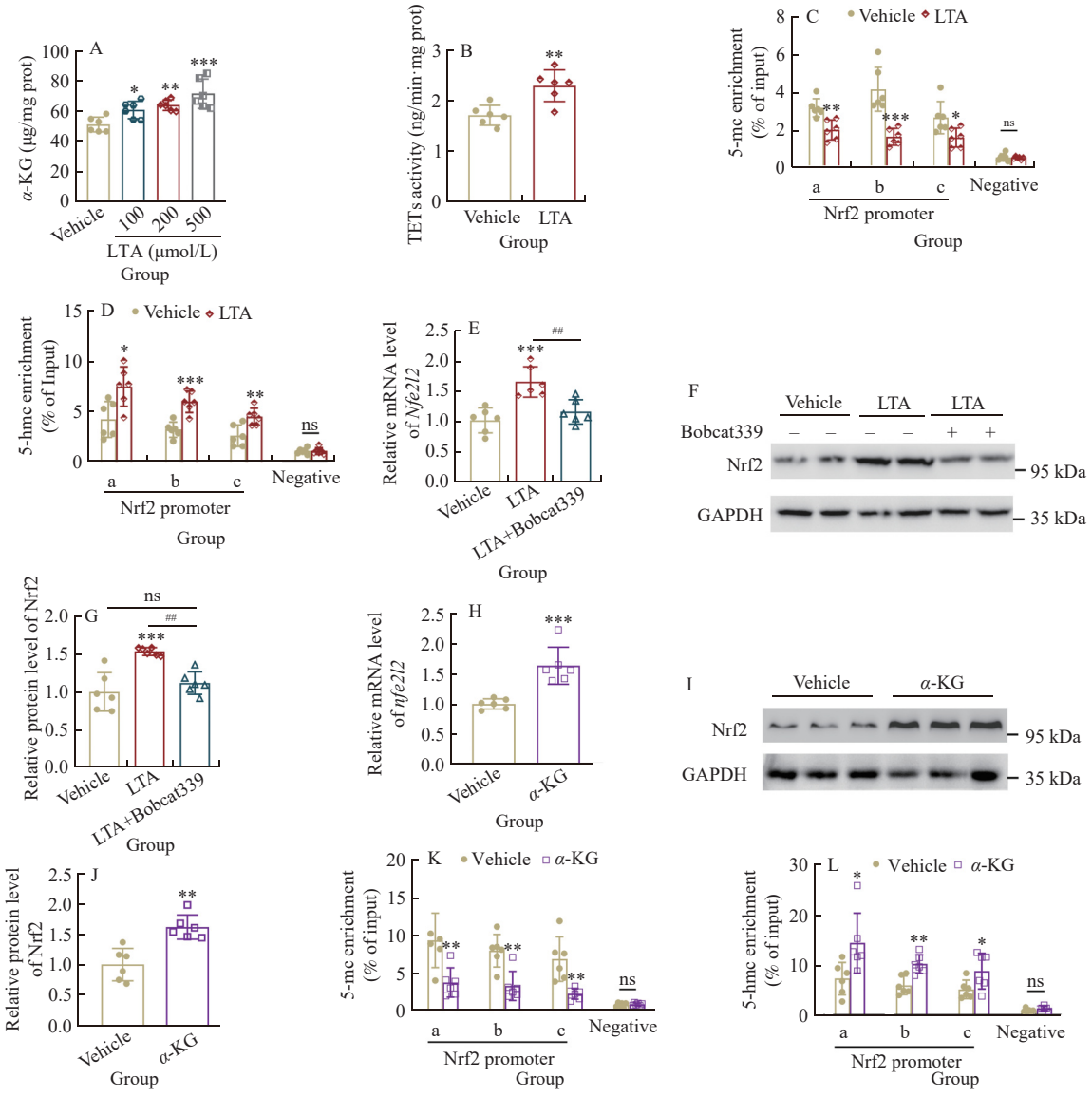

Fig. 7 LTA increases the cellular content of α-KG and decreases the DNA methylation level of Nrf2 promoter in hepatocytes. (A) Level of α-KG in primary hepatocytes. (B) Activity of TETs in primary hepatocytes. Enrichment levels of (C) 5-mc and (D) 5-hmc on the *Nrf2* promoter in primary hepatocytes. Prior to LTA intervention, cells were pretreated with Bobcat339, an inhibitor of TETs, for 2 h. (E) mRNA levels of the indicated genes in mice primary hepatocytes (F) Immunoblotting analysis of the proteins. (G) Quantification of immunoblotting results. (H) mRNA levels of the indicated genes in mice primary hepatocytes. (I) Immunoblotting analysis of the proteins. (J) Quantification of immunoblotting results. Enrichment levels of (K) 5-mc and (L) 5-hmc on the Nrf2 promoter in primary hepatocytes. 200 μmol/L LTA was used. One-way analysis of variance plus Tukey's post hoc tests were performed in (A, E and G); unpaired two-tailed *t*-tests was performed in (B, H and J); two-way analysis of variance plus Tukey's post hoc tests were performed in (C, D, K and L). All data show the means ± SD, $n = 6$. $^{*}P < 0.05$, $^{**}P < 0.01$, $^{***}P < 0.001$, comparing to the vehicle group. $^{\#\#}P < 0.01$. ns. no significant difference.

protein expression of Nrf2. Consistently, α-KG attenuated the 5-mc level on the 3 promoters of *Nrf2* and increased the 5-hmc level (Figs. 7K and L). These results indicate that α-KG-mediated demethylation of *Nrf2* promoter may be involved in LTA-induced *Nrf2* expression. Overall, the above *in vivo* experiments indicate that LTA promotes DNA demethylation of the *Nrf2* gene promoter to facilitate Nrf2 expression by upregulating the cellular level of α-KG in hepatocytes.

4. Discussion

In this study, the role of exercise and LTA in ameliorating NASH was investigated in GAN diet-induced NASH mouse model. It was found exercise and LTA had synergistic effects on the alleviation of obesity-related metabolic disorders, hepatic steatosis and liver injury, in which up-regulation of Nrf2 expression and Nrf2-mediated anti-oxidative responses was involved. At the mechanistic level, both exercise and LTA can significantly induce the upregulation of hepatic α-KG level, and the combination of exercise and LTA intervention led to a significant higher elevation of hepatic α-KG level. The α-KG can decrease the 5-mc level and increase 5-hmc level on *Nrf2* promoter region by upregulating TETs activity, ultimately leading to increased Nrf2 transcriptional expression. Therefore, the combination of LTA and exercise may provide a more efficient way to prevent NASH.

LTA has multifaceted health benefits. For example, LTA has been reported to improve cognitive ability, protect neurons against

neurotoxic agents, counteract blood pressure increase, improve immune function and promote white adipocytes browning[28]. Notably, the specific role and mechanism of LTA in NASH remains not well defined. In this study, we showed that LTA enhanced the liver antioxidant function, contributing to improvement in obesity, enhanced insulin sensitivity, and reduced hepatic fibrosis in mice fed a GAN diet (Figs. 2 and 3). Furthermore, our *in vivo* studies using primary hepatocytes and HepG2 cells revealed that LTA directly induced the upregulation of Nrf2 *via* the α-KG/TETs/DNA demethylation pathway (Fig. 7). This provides strong evidence for the antioxidant function of LTA and also increases data support for the potential of LTA in the prevention and treatment of NASH.

Previous studies have highlighted that both high-intensity interval training (HIIT) and moderate intensity training (MIT) improve overall metabolic parameters and impede the progression of NASH by reducing hepatic triglycerides, inflammation and fibrosis. Mechanistically, exercise curtails the expression of fatty acid synthesis genes in the liver, subsequently reducing fatty acid production. Moreover, exercise shields the liver from NASH by diminishing the accumulation and activation of monocyte-derived macrophages. Exercise have also been shown to improve liver fat and histological severity in patients with NAFLD. Effective weight management is a key strategy for the management of NASH, with the most significant improvement observed in patients achieving weight loss of 10% or more[52]. This includes notable rates of NAFLD activity score (NAS) reduction, NASH resolution and fibrosis regression[53]. However, this magnitude of weight loss is difficult to achieve and harder to sustain. Due to low patient compliance, it is difficult for exercise in people's real life to achieve the effect in animals' exercise experiments, the practical application of exercise in the clinical realm for preventing and treating NASH still faces challenges and is not yet optimally realized[54]. Therefore, it is necessary to find a way to improve the effect of exercise or reduce the difficulty of exercise execution. In this study, we combined exercise and LTA to further increase the beneficial effects of exercise or LTA intervention on alleviating NASH phenotypes in mice. Exercise or LTA intervention can effectively ameliorate lipid accumulation, insulin resistance, liver damage, inflammation and fibrosis in mice (Figs. S2 and 3). Moreover, the combination of exercise and LTA intervention led to a significant further amelioration of NASH phenotypes. This may provide new measures for enhancing the effect of exercise in the prevention and control of NASH.

Understanding the signaling mechanisms that mitigate pathophysiological insults and uphold hepatocyte health in NASH remains a complex and insufficiently elucidated area. The progression of NASH is attributed to a combination of multiple parallel hits. This encompasses genetic variations, insulin resistance, and alterations in the intestinal microbiota. These multiple hits trigger endoplasmic reticulum (ER) stress and oxidative stress at the cellular level, and endocrine dysregulation, ultimately leading to the development of hepatic steatosis, inflammation, and fibrosis. Among these factors, oxidative stress is notably recognized as a pivotal contributor to the transition from simple fatty liver to NASH[52]. Lack of antioxidant enzymes led to increased oxidative stress and liver injury in mice, which further progressed to spontaneous hepatocellular carcinoma (HCC) with age. Oxidative stress plays a role in the progression of simple fatty liver to NASH[55-56]. Slowing down the progression of NASH and fibrosis involves interventions aimed at modulating hepatic oxidative stress and mitigating mitochondrial dysfunction[57]. The above study provides compelling evidence that underscores the pivotal role of hepatic oxidative stress and mitochondrial dysfunction in the occurrence of hepatocyte death, steatosis, inflammation and liver fibrosis in the context of NASH. In our study, LTA induces α-KG upregulation in hepatocytes (Fig. 7). In consistence with this, LTA intervention alone was also effective in increasing the level of α-KG in the liver of NASH mice (Fig. 4G). Interestingly, upregulation of α-KG was also demonstrated after exercise alone, and the combined intervention showed a more efficient effect in increasing α-KG level (Fig. 4G). The function of α-KG has been reported to be a cofactor for TETs catalyzing DNA demethylation. Therefore, we propose that LTA-induced upregulation of α-KG eventually promotes the TETs-mediated demethylation of the *Nrf2* promoter. Indeed, our results did show that LTA catalyzes the demethylation of the *Nrf2* promoter by increasing TETs activity through α-KG. LTA-induced upregulation of *Nrf2* transcription levels and protein levels was confirmed in both hepatocytes and NASH mice livers (Figs. 4 and 7). Taken together, our results reveal an LTA/α-KG/Nrf2 axis that promotes antioxidant action in the liver, which helps to halt NASH.

Our results indicate that both exercise and LTA could increase the α-KG level in the liver, which promotes Nrf2 expression by facilitating TETs-mediated demethylation of *Nrf2* promoter. Exercise can promote the production of α-KG in muscle, which can be released from the muscle into the blood, thereby increasing the serum α-KG level[58]. The increased serum α-KG level may indirectly upregulate the α-KG level in the liver because of the increased uptake of α-KG from the blood by liver cells. Within the cells, LTA could be catabolized to produce ethylamine and glutamate[25,59], which may promote the production of α-KG from glutamate. LTA may increase intracellular α-KG level through the above way. Therefore, exercise and LTA could lead to the increase of α-KG level in hepatocytes by different mechanism. Further studies are needed to dissect the exact mechanism of how LTA and exercise lead to the upregulation of α-KG in hepatocytes.

Our results show an additive effect of exercise and LTA in ameliorating NASH. We identify that LTA and exercise can synergistically promote the expression of Nrf2 in hepatocytes through the α-KG/TETs/DNA demethylation pathway, which enhances the Nrf2-mediated the anti-oxidative responses in the liver, thereby inhibiting liver injury (Fig. 8).

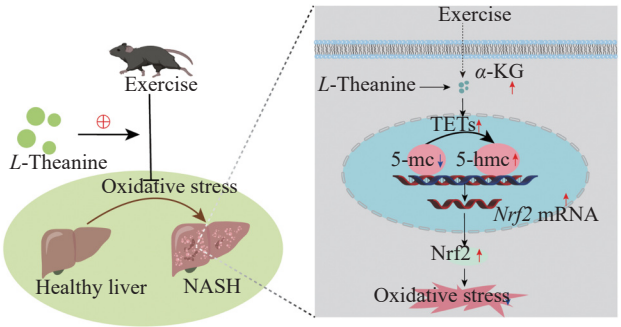

Fig. 8 LTA and exercise synergistically improve NASH through the α-KG/Nrf2 axis. LTA and exercise together appear to show a synergistic effect on halting NASH progression. At the mechanistic level, LTA and exercise synergistically promote hepatic α-KG level, which increases the 5-hmc levels on *Nrf2* gene promoter by upregulating TETs activity, ultimately leading to increased *Nrf2* transcription. The above process blunts the oxidative stress in the liver, thereby ameliorating diet-induced NASH in mice.

In conclusion, the combination of LTA and exercise may provide an effective measure for the prevention and control of NASH, in which the α-KG/Nrf2 axis-mediated anti-oxidative pathway is involved. It should be noted that other pathways may also contribute to the amelioration of NASH by exercise and LTA, which warrants further investigation. Collectively, our results demonstrate that the combination of LTA and exercise may provide an approach to help alleviate NASH.

Conflict of interest

All authors disclosed no relevant relationships. The authors declared no potential conflicts of interest with respect to the research, author ship, and/or publication of this article.

Acknowledgements

This work was supported by the National Natural Science Foundation of China (82571021, 32070751 and 31871435), the Shanghai Natural Science Foundation (25ZR1401328), and the Program for Overseas High-level talents at Shanghai Institutions of Higher Learning (TP2022100).

Appendix A. Supplementary information

Supplementary data associated with this article can be found, in the online version, at http://doi.org/10.26599/FSHW.2024.9250242.

References

[1] E.E. Powell, V.W. Wong, M. Rinella, Non-alcoholic fatty liver disease, Lancet 397 (2021) 2212-2224. https://doi.org/10.1016/S0140-6736(20)32511-3.

[2] N. Chalasani, Z. Younossi, J.E. Lavine, et al., The diagnosis and management of nonalcoholic fatty liver disease: practice guidance from the American Association for the Study of Liver Diseases, Hepatology 67 (2018) 328-357. https://doi.org/10.1002/hep.29367.

[3] G.T. Brown, D.E. Kleiner, Histopathology of nonalcoholic fatty liver disease and nonalcoholic steatohepatitis, Metabolism 65 (2016) 1080-1086. https://doi.org/10.1016/j.metabol.2015.11.008.

[4] Y. Li, L. Guo, The versatile role of Serpina3c in physiological and pathological processes: a review of recent studies, Front. Endocrinol. 14 (2023) 1189007. https://doi.org10.3389/fendo.2023.1189007.

[5] H.Y. Luo, J.Y. Zhu, M. Chen, et al., Kruppel-like factor 10 (KLF10) as a critical signaling mediator: versatile functions in physiological and pathophysiological processes, Genes Dis. 10 (2023) 915-930. https://doi.org/10.1016/j.gendis.2022.06.005.

[6] M. Chen, J.Y. Zhu, W.J. Mu, et al., Cysteine dioxygenase type 1 (CDO1): Its functional role in physiological and pathophysiological processes, Genes Dis. 10 (2023) 877-890. https://doi.org10.1016/j.gendis.2021.12.023.

[7] M. Chen, J.Y. Zhu, W.J. Mu, et al., The journey towards physiology and pathology: tracing the path of neuregulin 4, Genes Dis. 11 (2024) 687-700. https://doi.org/10.1016/j.gendis.2023.03.021.

[8] S. Li, L. Guo, The role of Sirtuin 2 in liver - an extensive and complex biological process, Life. Sci. 339 (2024) 122431. https://doi.org/10.1016/j.lfs.2024.122431.

[9] A.C. Sheka, O. Adeyi, J. Thompson, et al., Nonalcoholic steatohepatitis: a review, JAMA 323 (2020) 1175-1183. https://doi.org/10.1001/jama.2020.2298.

[10] R. Carrie, Wong K. Lim, The association between nonalcoholic fatty liver disease and cardiovascular disease outcomes, Clinical Liver Disease 12 (2018) 39-44. https://doi.org/10.1002/cld.721.

[11] Z.M. Younossi, M. Stepanova, N. Rafiq, et al., Nonalcoholic steatofibrosis independently predicts mortality in nonalcoholic fatty liver disease, Hepatol. Commun. 1 (2017) 421-428. https://doi.org/10.1002/hep4.1054.

[12] P.S. Dulai, S. Singh, J. Patel, et al., Increased risk of mortality by fibrosis stage in nonalcoholic fatty liver disease: systematic review and meta-analysis, Hepatology 65 (2017) 1557-1565. https://doi.org/10.1002/hep.29085.

[13] P.S. Dulai, S. Singh, J. Patel, et al., Predictors of all-cause mortality and liver-related mortality in patients with non-alcoholic fatty liver disease (NAFLD), Dig. Dis. Sci. 58 (2013) 3017-3023. https://doi.org/10.1007/s10620-013-2743-5.

[14] Z.M. Younossi, M. Stepanova, J. Ong, et al., Nonalcoholic steatohepatitis is the most rapidly increasing indication for liver transplantation in the United States, Clin. Gastroenterol. Hepatol. 19 (2021) 580-589 e585. https://doi.org/10.1016/j.cgh.2020.05.064.

[15] C. Estes, Q.M. Anstee, M.T. Arias-Loste, et al., Modeling NAFLD disease burden in China, France, Germany, Italy, Japan, Spain, United Kingdom, and United States for the period 2016–2030, J. Hepatol. 69 (2018) 896-904. https://doi.org/10.1016/j.jhep.2018.05.036.

[16] L. Yan, L. Guo, Exercise-regulated white adipocyte differentitation: an insight into its role and mechanism, J. Cell. Physiol. 238 (2023) 1670-1692. https://doi.org/10.1002/jcp.31056.

[17] W.J. Mu, J.Y. Zhu, M. Chen, et al., Exercise-mediated browning of white adipose tissue: its significance, mechanism and effectiveness, Int. J. Mol. Sci. 22 (2021) 11512. https://doi.org/10.3390/ijms222111512.

[18] D.J. Windt, V. Sud, H. Zhang, et al., The effects of physical exercise on fatty liver disease, Gene. Expr. 18 (2018) 89-101. https://doi.org/10.3727/105221617X15124844266408.

[19] M. Chen, J.Y. Zhu, W.J. Mu, et al., Cdo1-Camkk2-AMPK axis confers the protective effects of exercise against NAFLD in mice, Nat. Commun. 14 (2023) 8391. https://doi.org/10.1038/s41467-023-44242-7.

[20] A.S. George, A. Bauman, A. Johnston, et al., Independent effects of physical activity in patients with nonalcoholic fatty liver disease, Hepatology 50 (2009) 68-76. https://doi.org/10.1002/hep.22940.

[21] A.M. Hoek, J.C. Jong, N. Worms, et al., Diet and exercise reduce pre-existing NASH and fibrosis and have additional beneficial effects on the vasculature, adipose tissue and skeletal muscle *via* organ-crosstalk, Metabolism 124 (2021) 154873. https://doi.org/10.1016/j.metabol.2021.154873.

[22] V.W. Wong, G.L. Wong, R.S. Chan, et al., Beneficial effects of lifestyle intervention in non-obese patients with non-alcoholic fatty liver disease, J. Hepatol. 69 (2018) 1349-1356. https://doi.org/10.1016/j.jhep.2018.08.011.

[23] C.S. Baba, G. Alexander, B. Kalyani, et al., Effect of exercise and dietary modification on serum aminotransferase levels in patients with nonalcoholic steatohepatitis, J. Gastroenterol. Hepatol. 21 (2006) 191-198. https://doi.org/10.1111/j.1440-1746.2005.04233.x.

[24] H. Tsuge, S. Sano, T. Hayakawa, et al., Theanine, gamma-glutamylethylamide, is metabolized by renal phosphate-independent glutaminase, Biochim Biophys. Acta 1620 (2003) 47-53. https://doi.org/10.1016/s0304-4165(02)00504-4.

[25] S. Lin, Z. Chen, T. Chen, et al., Theanine metabolism and transport in tea plants (*Camellia sinensis* L.): advances and perspectives, Crit. Rev. Biotechnol. 43 (2023) 327-341. https://doi.org/10.1080/07388551.2022.2036692.

[26] J. Zhao, P. Li, T. Xia,et al., Exploring plant metabolic genomics: chemical diversity, metabolic complexity in the biosynthesis and transport of specialized metabolites with the tea plant as a model, Crit. Rev. Biotechnol. 40 (2020) 667-688. https://doi.org/10.1080/07388551.2020.1752617.

[27] S. Kitaoka, H. Hayashi, H. Yokogoshi, et al., Transmural potential changes associated with the *in vitro* absorption of theanine in the guinea pig intestine, Biosci. Biotechnol. Biochem. 60 (1996) 1768-1771. https://doi.org/10.1271/bbb.60.1768.

[28] J. Williams, D. Sergi, A.J. McKune, et al., The beneficial health effects of green tea amino acid *L*-theanine in animal models: promises and prospects for human trials, Phytother. Res. 33 (2019) 571-583. https://doi.org/10.1002/ptr.6277.

[29] J. Liang, L. Gu, X. Liu, et al., *L*-Theanine prevents progression of nonalcoholic hepatic steatosis by regulating hepatocyte lipid metabolic pathways *via* the CaMKKbeta-AMPK signaling pathway, Nutr. Metab. 19 (2022) 29. https://doi.org/10.1186/s12986-022-00664-6.

[30] G. Li, Y. Ye, J. Kang, et al., *L*-Theanine prevents alcoholic liver injury through enhancing the antioxidant capability of hepatocytes, Food Chem. Toxicol. 50 (2012) 363-372. https://doi.org/10.1016/j.fct.2011.10.036.

[31] K. Nagai, A. Oda, H. Konishi, Theanine prevents doxorubicin-induced acute hepatotoxicity by reducing intrinsic apoptotic response, Food Chem. Toxicol. 78 (2015) 147-152. https://doi.org/10.1016/j.fct.2015.02.009.

[32] J.J. Fu , F.J. Hu, T.F. Ma, et al., A conventional immune regulator mitochondrial antiviral signaling protein blocks hepatic steatosis by maintaining mitochondrial homeostasis, Hepatology 75 (2022) 403-418. https://doi.org/10.1002/hep.32126.

[33] Y.Y. Guo, B.Y. Li, G. Xiao, et al., Cdo1 promotes PPARγ-mediated adipose tissue lipolysis in male mice, Nat. Metab. 4 (2022) 1352-1368. https://doi.org/10.1038/s42255-022-00644-3.

[34] Y.Y. Guo, B.Y. Li, W.Q. Peng, et al., Taurine-mediated browning of white adipose tissue is involved in its anti-obesity effect in mice, J. Biol. Chem. 294 (2019) 15014-15024. https://doi.org/10.1074/jbc.RA119.009936.

[35] L. Guo, P. Zhang, Z.M. Chen, et al., Hepatic neuregulin 4 signaling defines an endocrine checkpoint for steatosis-to-NASH progression. J. Clin. Invest. 127 (2017) 4449-4461, https://doi.org/10.1172/JCI96324.

[36] B.Y. Li, W.Q. Peng, Y. Liu, et al., HIGD1A links SIRT1 activity to adipose browning by inhibiting the ROS/DNA damage pathway, Cell Rep. 42 (2023) 112731. https://doi.org/10.1016/j.celrep.2023.112731.

[37] J.Y. Zhu, M. Chen, W.J. Mu, et al., Higd1a facilitates exercise-mediated alleviation of fatty liver in diet-induced obese mice, Metabolism 134 (2022) 155241. https://doi.org10.1016/j.metabol.2022.155241.

[38] L. Guo, S.R. Zhou, X.B. Wei, et al., Acetylation of mitochondrial trifunctional protein alpha-subunit enhances its stability to promote fatty acid oxidation and is decreased in nonalcoholic fatty liver disease, Mol. Cell. Biol. 36 (2016) 2553-2567. https://doi.org10.1128/MCB.00227-16.

[39] B.Y. Li, Y.Y. Guo, G. Xiao, et al., SERPINA3C ameliorates adipose tissue inflammation through the Cathepsin G/Integrin/AKT pathway, Mol. Metab. 61 (2022) 101500. https://doi.org10.1016/j.molmet.2022.101500.

[40] L. Guo, Y.Y. Guo, B.Y. Li, et al., Histone demethylase KDM5A is transactivated by the transcription factor C/EBPβ and promotes preadipocyte differentiation by inhibiting Wnt/*β*-catenin signaling, J. Biol. Chem. 294 (2019) 9642-9654. https://doi.org10.1074/jbc.RA119.008419.

[41] Y. Liu, W. Q. Peng, Y.Y. Guo, et al., Kruppel-like factor 10 (KLF10) is transactivated by the transcription factor C/EBPβ and involved in early 3T3-L1 preadipocyte differentiation, J. Biol. Chem. 293 (2018) 14012-14021. https://doi.org10.1074/jbc.RA118.004401.

[42] J.S. Lim, M. Mietus-Snyder, A. Valente, et al., The role of fructose in the pathogenesis of NAFLD and the metabolic syndrome, Nat. Rev. Gastroenterol. Hepatol. 7 (2010) 251-264. https://doi.org10.1038/nrgastro.2010.41.

[43] N. Alkhouri, L.J. Dixon, A.E. Feldstein, Lipotoxicity in nonalcoholic fatty liver disease: not all lipids are created equal, Expert. Rev. Gastroenterol. Hepatol. 3 (2009) 445-451. https://doi.org10.1586/egh.09.32.

[44] M.B. Møllerhøj, S.S. Veidal, K.T. Thrane, et al., Hepatoprotective effects of semaglutide, lanifibranor and dietary intervention in the GAN diet-induced obese and biopsy-confirmed mouse model of NASH, Clin. Transl. Sci. 15 (2022) 1167-1186. https://doi.org10.1111/cts.13235.

[45] C.H. Wang, C.Y. Cui, H. Li, et al., Nrf2 deletion causes “benign” simple steatosis to develop into nonalcoholic steatohepatitis in mice fed a high-fat diet, Lipids Health Dis. 12 (2013) 165. https://doi.org10.1186/1476-511X-12-165.

[46] K. Okada, E. Warabi, H. Sugimoto, et al,. Deletion of Nrf2 leads to rapid progression of steatohepatitis in mice fed atherogenic plus high-fat diet, J. Gastroenterol. 48 (2013) 620-632. https://doi.org10.1007/s00535-012-0659-z.

[47] Q.Y. Yang, X.W. Liang, X.F. Sun, et al., AMPK/*α*-ketoglutarate axis dynamically mediates DNA demethylation in the Prdm16 promoter and brown adipogenesis, Cell Metab. 24 (2016) 542-554. https://doi.org10.1016/j.cmet.2016.08.010.

[48] W.Q. Peng, G. Xiao, B.Y. Li, et al., *L*-Theanine activates the browning of white adipose tissue through the AMPK/*α*-ketoglutarate/Prdm16 axis and ameliorates diet-induced obesity in mice, Diabetes 70 (2021) 1458-1472. https://doi.org10.2337/db20-1210.

[49] J. Zhang, S.D. Zhang, P. Wang, et al., Pinolenic acid ameliorates oleic acid-induced lipogenesis and oxidative stress *via* AMPK/SIRT1 signaling pathway in HepG2 cells, Eur. J. Pharmacol. 861 (2019) 172618. https://doi.org10.1016/j.ejphar.2019.172618.

[50] Y. Rao, Y.T. Lu, C. Li, et al., Bouchardatine analogue alleviates non-alcoholic hepatic fatty liver disease/non-alcoholic steatohepatitis in high-fat fed mice by inhibiting ATP synthase activity, Br. J. Pharmacol. 176 (2019) 2877-2893. https://doi.org10.1111/bph.14713.

[51] A. Akoumi, T. Haffar, M. Mousterji, et al., Palmitate mediated diacylglycerol accumulation causes endoplasmic reticulum stress, Plin2 degradation, and cell death in H9C2 cardiomyoblasts, Exp. Cell. Res. 354 (2017) 85-94. https://doi.org10.1016/j.yexcr.2017.03.032.

[52] A. Takaki, D. Kawai, K. Yamamoto, Multiple hits, including oxidative stress, as pathogenesis and treatment target in non-alcoholic steatohepatitis (NASH), Int. J. Mol. Sci. 14 (2013) 20704-20728. https://doi.org10.3390/ijms141020704.

[53] V.G. Eduardo, M.P. Yadina, C.B. Luis, et al., Weight loss through lifestyle modification significantly reduces features of nonalcoholic steatohepatitis, Gastroenterology 149 (2015) 367-378. https://doi.org10.1053/j.gastro.2015.04.005.

[54] L. Guo, Y.Y. Guo, B.Y. Li, et al., Enhanced acetylation of ATP-citrate lyase promotes the progression of nonalcoholic fatty liver disease, J. Biol. Chem. 294 (2019) 11805-11816, https://doi.org10.1074/jbc.RA119.008708.

[55] J.Y. Zhu, M. Chen, W.J. Mu, et al., The functional role of Higd1a in mitochondrial homeostasis and in multiple disease processes, Genes Dis. 10 (2023) 1833-1845. https://doi.org10.1016/j.gendis.2022.03.018.

[56] S. Mohammed, E.H. Nicklas, N. Thadathil, et al., Role of necroptosis in chronic hepatic inflammation and fibrosis in a mouse model of increased oxidative stress, Free. Radic. Biol. Med. 164 (2021) 315-328. https://doi.org10.1016/j.freeradbiomed.2020.12.449.

[57] S.Y. Li, X. Li, F.Y. Chen, et al., Nobiletin mitigates hepatocytes death, liver inflammation, and fibrosis in a murine model of NASH through modulating hepatic oxidative stress and mitochondrial dysfunction, J. Nutr. Biochem. 100 (2022) 108888. https://doi.org10.1016/j.jnutbio.2021.108888.

[58] Y.X. Yuan, P.W. Xu, Q.Y. Jiang, et al., Exercise-induced alpha-ketoglutaric acid stimulates muscle hypertrophy and fat loss through OXGR1-dependent adrenal activation, EMBO. J. 39 (2020) e103304. https://doi. org10.15252/embj.2019103304.

[59] X.M. Fu, S.H. Cheng, Y.Y. Liao, et al., Characterization of *L*-theanine hydrolase *in vitro* and subcellular distribution of its specific product ethylamine in tea (*Camellia sinensis*), J. Agric. Food Chem. 68 (2020) 10842-10851. https://doi.org10.1021/acs.jafc.0c01796.